This is a repository copy of *Gradient based sequential Markov chain Monte Carlo for multitarget tracking with correlated measurements*.

White Rose Research Online URL for this paper:
http://eprints.whiterose.ac.uk/120920/

Version: Published Version

Article:
Lamberti, R., Septier, F., Salman, N. et al. (1 more author) (2018) Gradient based sequential Markov chain Monte Carlo for multitarget tracking with correlated measurements. IEEE Transactions on Signal and Information Processing over Networks, 4 (3). pp. 510-518. ISSN 2373-776X

https://doi.org/10.1109/TSIPN.2017.2756563

Reuse
This article is distributed under the terms of the Creative Commons Attribution (CC BY) licence. This licence allows you to distribute, remix, tweak, and build upon the work, even commercially, as long as you credit the authors for the original work. More information and the full terms of the licence here: https://creativecommons.org/licenses/

Takedown
If you consider content in White Rose Research Online to be in breach of UK law, please notify us by emailing eprints@whiterose.ac.uk including the URL of the record and the reason for the withdrawal request.

eprints@whiterose.ac.uk
https://eprints.whiterose.ac.uk/

Gradient-Based Sequential Markov Chain Monte Carlo for Multitarget Tracking With Correlated Measurements

Roland Lamberti, François Septier, Naveed Salman, and Lyudmila Mihaylova, *Senior Member, IEEE*

***Abstract*—Measurements in wireless sensor networks (WSNs) are often correlated both in space and in time. This paper focuses on tracking multiple targets in WSNs by taking into consideration these measurement correlations. A sequential Markov Chain Monte Carlo (SMCMC) approach is proposed in which a Metropolis within Gibbs refinement step and a likelihood gradient proposal are introduced. This SMCMC filter is applied to case studies with cellular network received signal strength data in which the shadowing component correlations in space and time are estimated. The efficiency of the SMCMC approach compared to particle filtering, as well as the gradient proposal compared to a basic prior proposal, are demonstrated through numerical simulations. The accuracy improvement with the gradient-based SMCMC is above 90% when using a low number of particles. Thanks to its sequential nature, the proposed approach can be applied to various WSN applications, including traffic mobility monitoring and prediction.**

***Index Terms*—Multiple target tracking, correlated shadowing, sequential Markov Chain Monte Carlo (SMCMC), gradient-based likelihood proposal.**

I. Introduction

TRACKING multiple mobile targets is a challenging task which has applications in a number of fields, including that of wireless cellular communication networks and mobility prediction for intelligent transportation systems. In this area, the main structure of a system will feature target nodes whose kinematic states are unknown and need to be estimated; and sensor nodes receiving some type of noisy information about the target nodes, from which an estimation of their states can be inferred.

A variety of methods have been developed in order to solve this localization problem. The more common range-based methods (as opposed to range-free methods) depend on the distances between nodes, through measurements of received signal strengths (RSS), signal time-of-arrivals (ToA) [1] or angle-of-arrivals (AoA) [2] originating from the targets. Both ToA and AoA approaches allow for accurate distance estimations leading to good localization, however ToA requires synchronized clocks on the target nodes, while AoA requires an array of antennas and is still sensitive to errors due to multipath, making them costly solutions. The received signal strength technique [3] is a much more direct and simple approach, with low implementation costs; as such, it is a recurrent subject of performance optimization attempts. Taking into account the shadowing correlation (Gudmunson's model [4], [5]) between different nodes (targets or sensors), which capitalizes on the fact that in a given environment, closeby areas present more or less similar behaviors with regard to shadowing, and may thus be modeled as highly correlated, is one such way of improving this technique. A few examples of research include [6] which studies the combination of measurement correlation and shrinkage estimation of the covariance matrix for significant performance improvements, but is limited to the static case. In [7]–[10] the measurement correlations are taken into account and refined particle filtering (or Sequential Importance Resampling - SIR) algorithms are implemented. This results in high localization accuracy, however these algorithms inherently suffer from the limitations of the particle filtering approach. Although this approach is known to be an effective way of solving non-linear problems, it performs poorly in high-dimensional state-spaces [11].

In this paper, we present a novel Bayesian solution to tracking problems with correlated measurements based on an advanced Monte-Carlo algorithm. Firstly, we take into account the shadowing correlations both spatially and in time, that is, between either current or past positions of any targets. This allows for performance improvements both due to the correlations in time between positions of a single target, and due to the correlations between trajectories of different targets which may cross at some point in time. Finally, in order to efficiently solve the Bayesian tracking problem, we propose to use a Sequential Markov Chain Monte Carlo (SMCMC) algorithm. This technique, which is still largely under-exploited in the signal processing literature, allows for more robust and overall better performance than the more classical particle filtering, especially in high-dimensional systems [12]–[14]. The combination of these two features thus

Manuscript received September 22, 2016; revised May 2, 2017 and July 24, 2017; accepted September 5, 2017. Date of publication September 25, 2017; date of current version August 7, 2018.This work is supported by the UK Engineering and Physical Sciences Research Council (EPSRC) via the Bayesian Tracking and Reasoning over Time (BTaRoT) under Grant EP/K021516/1. The associate editor coordinating the review of this manuscript and approving it for publication was Dr. Marcelo Bruno. *(Corresponding author: Roland Lamberti.)*

R. Lamberti is with the IMT Télécom Sudparis, Univ. Paris-Saclay, CNRS UMR 5157 - SAMOVAR, Evry 91011, France (e-mail: roland.lamberti@telecom-sudparis.eu).

F. Septier is with the IMT Lille Douai, Univ. Lille, CNRS UMR 9189 - CRIStAL, Lille F-59000, France (e-mail: francois.septier@telecom-lille.fr).

N. Salman and L. Mihaylova are with the University of Sheffield, Sheffield S10 2TN, U.K. (e-mail: n.salman@sheffield.ac.uk; L.S.Mihaylova@sheffield.ac.uk).

Digital Object Identifier 10.1109/TSIPN.2017.2756563

This work is licensed under a Creative Commons Attribution 3.0 License. For more information, see http://creativecommons.org/licenses/by/3.0/

has a good potential for overall robustness in tracking performance in a wide range of scenarios. Preliminary results, including experimental analyses regarding the benefits of taking into account the spatio-temporal shadowing correlation, are already reported in our previous work [15]. We now detail and justify our choice of the SMCMC methodology and complete these results by replacing the prior proposal density of the Gibbs refinement step with a likelihood gradient proposal. This allows to better capitalize on informative measurements and guides the particles towards high-likelihood zones, increasing the efficiency of the algorithm. Finally, we present new simulation results demonstrating the benefits of this distribution over the prior and further justifying the superiority of SMCMC over SIR in our model, when both have similar sampling costs and use the same proposal densities.

The paper is structured as follows. Section II details the choice of the target and observation models. Section III-B explains the Bayesian framework used as well as the SMCMC solution, and Section IV details how to integrate the likelihood gradient in the proposal density of the Gibbs refinement step. Simulation results using synthetic data on the superiority of SMCMC with Gibbs refinement compared to SIR with resample-move, and the benefits of this gradient proposal compared to the prior, are presented and analyzed in Section V, while Section VI highlights the main conclusions of this work.

II. Target and Observation Models

A. Target State and Motion Models

In a 2-dimensional (2-D) network, the kinematic state of a single target at discrete time step t may be defined as a vector of positions and velocities $\mathbf{x}_t = [x_{t,x}, x_{t,y}, x_{t,\dot{x}}, x_{t,\dot{y}}]^T$, although it could also contain accelerations or other variables of interest. Here, $\mathbb{N}^*$ represents the set of all natural numbers excluding 0; the kinematic state $\{\mathbf{x}_{t,1:N}\}_{t\in\mathbb{N}^*} = \{[(\mathbf{x}_{t,1})^T, (\mathbf{x}_{t,2})^T, \ldots, (\mathbf{x}_{t,N})^T]\}_{t\in\mathbb{N}^*}$ of a set of N targets is considered to be a stochastic Markov process such that at any time step t, the transition probability density function (pdf) $p(\mathbf{x}_{t,1:N}|\mathbf{x}_{1:t-1,1:N}) = p(\mathbf{x}_{t,1:N}|\mathbf{x}_{t-1,1:N})$ is known and can either be evaluated point-wise or sampled from.

B. Correlated Observation Model

Consider a set of N targets evolving from time 1 to time T, $\mathbf{x}_{1:T,1:N}$, and a set of M immobile sensors $\mathbf{s} = [\mathbf{s}^1, \cdots, \mathbf{s}^M]$ where $\mathbf{s}^i = [s_x^i, s_y^i]^T$ is the position of the i-th sensor for $i \in \{1, \ldots, M\}$. We suppose that both N and M are fixed and known in this model. Throughout the paper, with the exception of square functions, superscripts will be used to denote a sensor i, a particle n or a Monte Carlo run l (in the simulations section), and subscripts will mostly be used to denote a time step t, a target j or a component $\{x, y, \dot{x}, \dot{y}\}$. At time $t \in \{1, \cdots, T\}$, a target $j \in \{1, \cdots, N\}$ transmitting a signal with power $P_{t,j}$ causes a sensor i to receive a signal with power $P_{t,j}^i$ (the data association problem is assumed to be resolved, for example it could be assumed that the targets emit during preassigned epochs). The corresponding path-loss can be expressed as

$$\mathcal{L}_{t,j}^i = 10\log_{10}\ P_{t,j} - 10\log_{10}\ P_{t,j}^i \tag{1}$$

The observed path-loss signal $y_{t,j}^i$ at the sensor can empirically be modeled [16]–[19] as

$$y_{t,j}^i = \mathcal{L}_{t,j}^i - \mathcal{L}_0 = 10\alpha\log_{10}\ d(\mathbf{x}_{t,j}, \mathbf{s}^i) + w_{t,j}^i \tag{2}$$

where

$$d(\mathbf{x}_{t,j}, \mathbf{s}^i) = \sqrt{(x_{t,j,x} - s_x^i)^2 + (x_{t,j,y} - s_y^i)^2} \tag{3}$$

corresponds to the Euclidean distance between the position of the j-th target at time t and the i-th sensor. $\mathcal{L}_0$ is the path-loss signal at a reference distance of usually 1 meter away from the sensor; α is the path-loss exponent (PLE) assumed known (or accurately estimated in a real application); and $w_{t,j}^i \sim \mathcal{N}(0, (\sigma_{t,j}^i)^2)$ is the realization of a random variable modeling the log-normal shadowing effect, with $\sigma_{t,j}^i$ the shadowing standard deviation associated with the link between the i-th sensor and the j-th target. Thus, the shadowing effect introduces a multiplicative factor in terms of distance which means the corresponding error induced is proportional to the distance itself. Therefore, this error will remain significant should the distance increase considerably. The standard deviation $\sigma_{t,j}^i$ is assumed to be constant over time, and we also consider the region of surveillance to be limited enough not to challenge the sensivity of the sensors.

In order to account for the spatio-temporal shadowing correlations between two positions within the network, we use the Gudmunson model [4]. Thus the correlation between the j-th target at time r and the k-th target at time t, for $(j,k) \in \{1, \ldots, N\}$ and $(r,t) \in \{1, \ldots, T\}$, is

$$Corr(\mathbf{x}_{r,j}, \mathbf{x}_{t,k}) = \exp\left(-\frac{d(\mathbf{x}_{r,j}, \mathbf{x}_{t,k})}{D_c}\right) \tag{4}$$

where D_c is the decorrelation distance used in the Gudmundson model, which depends on the environment (field measurements in [20] suggest values for D_c for different environments) and is assumed to be known or previously estimated.

By defining:

- $f^i(\mathbf{x}_{t,j}) = 10\alpha\log_{10}(d(\mathbf{x}_{t,j}, \mathbf{s}^i))$ the exact path-loss signal between the position of $\mathbf{x}_{t,j}$ and that of $\mathbf{s}^i$;
- $\rho^i(\mathbf{x}_{r,1:N}, \mathbf{x}_{t,1:N})$ a $N \times N$ matrix whose (j,k) term $[\rho^i(\mathbf{x}_{r,1:N}, \mathbf{x}_{t,1:N})]_{j,k} = \sigma_{r,j}^i\sigma_{t,k}^i \exp\left(-\frac{d(\mathbf{x}_{r,j}, \mathbf{x}_{t,k})}{D_c}\right)$ represents the covariance between the measurements at the i^{th} sensor corresponding to $\mathbf{x}_{r,j}$ and $\mathbf{x}_{t,k}$;

the collection of all the path-loss measurements observed at the i-th sensor until time t is then distributed according to the following multivariate Gaussian density $p(\mathbf{y}_{1:t,1:N}^i|\mathbf{x}_{1:t,1:N})$:

$$\mathbf{y}_{1:t,1:N}^i = \begin{bmatrix} y_{1,1}^i \\ \vdots \\ y_{1,N}^i \\ \vdots \\ y_{t,1}^i \\ \vdots \\ y_{t,N}^i \end{bmatrix} \sim \mathcal{N}\left(\begin{bmatrix} f^i(\mathbf{x}_{1,1}) \\ \vdots \\ f^i(\mathbf{x}_{1,N}) \\ \vdots \\ f^i(\mathbf{x}_{t,1}) \\ \vdots \\ f^i(\mathbf{x}_{t,N}) \end{bmatrix}, \mathbf{R}_t^i\right), \tag{5}$$

with $\mathbf{R}_t^i$ the $(N \times t, N \times t)$ observation covariance matrix which includes correlations in the measurements due to the close proximity of target positions, both "spatially" at a given time step and "spatio-temporally" between positions of different targets from different time steps, and can be expressed in blocks as:

$$\mathbf{R}_t^i = \begin{bmatrix} \rho^i(\mathbf{x}_{1,1:N}, \mathbf{x}_{1,1:N}) & \cdots & \rho^i(\mathbf{x}_{1,1:N}, \mathbf{x}_{t,1:N}) \\ \vdots & \ddots & \vdots \\ \rho^i(\mathbf{x}_{t,1:N}, \mathbf{x}_{1,1:N}) & \cdots & \rho^i(\mathbf{x}_{t,1:N}, \mathbf{x}_{t,1:N}) \end{bmatrix}. \quad (6)$$

Finally, measurements at each sensor are supposed to be independent from measurements at all other sensors - this is justified by considering scenarios where the sensor positions are immobile and sufficiently far apart from each other thus inducing little to no correlation. Thus the joint pdf of the measurements from several sensors can be calculated as the product of the pdfs of the measurements from each one of these sensors:

$$p(\mathbf{y}_{1:t,1:N}^{1:M} | \mathbf{x}_{1:t,1:N}) = \prod_{i=1}^{M} p(\mathbf{y}_{1:t,1:N}^{i} | \mathbf{x}_{1:t,1:N}). \quad (7)$$

III. Proposed Bayesian Solution

A. Recursive Inference

The aim of the Bayesian inference is to recursively estimate the states of the sequence of targets by computing the expectation of its joint posterior density. At time t, this posterior density can be deduced recursively as a function of its expression from the previous time step $t-1$:

$$\begin{aligned} p(\mathbf{x}_{1:t,1:N} | \mathbf{y}_{1:t,1:N}^{1:M}) \propto & \\ \prod_{i=1}^{M} p(\mathbf{y}_{t,1:N}^{i} | \mathbf{y}_{1:t-1,1:N}^{i}, \mathbf{x}_{1:t,1:N}) p(\mathbf{x}_{t,1:N} | \mathbf{x}_{t-1,1:N}) & \\ \times p(\mathbf{x}_{1:t-1,1:N} | \mathbf{y}_{1:t-1,1:N}^{1:M}). & \quad (8) \end{aligned}$$

However, this density is intractable mainly due to the nonlinear relationship of the hidden states in the observations and therefore needs to be approximated. In this posterior distribution of interest, the likelihood is obtained from (5) using classical conditional properties of the multivariate Gaussian distribution:

$$p(\mathbf{y}_{t,1:N}^{i} | \mathbf{y}_{1:t-1,1:N}^{i}, \mathbf{x}_{1:t,1:N}) = \mathcal{N}\left(\boldsymbol{\mu}_t^i, \boldsymbol{\Sigma}_t^i\right), \quad (9)$$

where

$$\begin{aligned} \boldsymbol{\mu}_t^i &= \boldsymbol{\mu}_2 + \boldsymbol{\Sigma}_{2,1} \boldsymbol{\Sigma}_{1,1}^{-1} (\mathbf{z} - \boldsymbol{\mu}_1), \\ \boldsymbol{\Sigma}_t^i &= \boldsymbol{\Sigma}_{2,2} - \boldsymbol{\Sigma}_{2,1} \boldsymbol{\Sigma}_{1,1}^{-1} \boldsymbol{\Sigma}_{1,2}, \end{aligned} \quad (10)$$

with

$$\begin{aligned} \mathbf{z} &= \mathbf{y}_{1:t-1,1:N}^{i}, \\ \boldsymbol{\mu}_1 &= [f^i(\mathbf{x}_{1,1}), \cdots, f^i(\mathbf{x}_{1,N}), \cdots, f^i(\mathbf{x}_{t-1,1}), \cdots, \\ &\quad f^i(\mathbf{x}_{t-1,N})]^T, \\ \boldsymbol{\mu}_2 &= [f^i(\mathbf{x}_{t,1}), \cdots, f^i(\mathbf{x}_{t,N})]^T, \\ \boldsymbol{\Sigma}_{1,1} &= \mathbf{R}_{t-1}^i, \\ \boldsymbol{\Sigma}_{2,1} &= [\rho^i(\mathbf{x}_{t,1:N}, \mathbf{x}_{1,1:N}), \cdots, \rho^i(\mathbf{x}_{t,1:N}, \mathbf{x}_{t-1,1:N})], \\ \boldsymbol{\Sigma}_{1,2} &= [\rho^i(\mathbf{x}_{1,1:N}, \mathbf{x}_{t,1:N}), \cdots, \rho^i(\mathbf{x}_{t-1,1:N}, \mathbf{x}_{t,1:N})]^T, \\ \boldsymbol{\Sigma}_{2,2} &= \rho^i(\mathbf{x}_{t,1:N}, \mathbf{x}_{t,1:N}). \end{aligned} \quad (11)$$

Given that any measurement is dependent on all of the other measurements at any time step, the sizes of the mean vector and covariance matrix of the observation defined in (5) grow with time. As a consequence, the cost of the computation of the likelihood in (9) that will be required in the filtering algorithm increases with time. In this paper, we therefore propose to use a strategy in order to have a constant computational cost by using a restriction of the size of the used history of positions, for instance through a sliding time window. One drawback of such an approximation is that it could imply the loss of interesting correlation information in cases where some targets approach past trajectories of some other targets (or themselves). Indeed, although the most significant correlations may often intuitively be the ones between positions of a same target at close time steps, simply due to their inherent proximity compared to the proximity of positions from different targets, this still depends on the chosen target motion model. It is likely to be the case if the targets move completely independently, which is clearly not always a correct assumption in real scenarios. However, the sliding time window approximation may also help in avoiding possible numerical problems in the evaluation of the likelihood (due to the inversion of a large covariance matrix). By defining the size of this sliding time window as t_{window}, the computation of the likelihood in (9) will involve a modified covariance matrix of size $(N \times (t_{\text{window}}+1), N \times (t_{\text{window}}+1))$ since $\forall (j,k) \in \{1, \ldots, N\}$, we will consider $Corr(\mathbf{x}_{r,j}, \mathbf{x}_{t,k}) = 0$ if $|r-t| > t_{\text{window}}$.

In a single target scenario, the authors in [10] propose to use a sequential Monte-Carlo method, known as particle filter, in order to infer the single target characteristics given the observations. However, this method suffers from intrinsic limitations in high-dimensional systems ([11], [21]), as the number of samples needs to increase exponentially with the variance of the weights (which is typically a linear function of the state dimension) so as to ensure that not only a single weight will be non-null. In order to obtain a more efficient algorithm for multiple target tracking, we thus propose an alternative solution based on a more advanced methodology known as Sequential Markov Chain Monte Carlo (SMCMC) [12].

B. The Proposed SMCMC Algorithm

Traditionally, Markov chain Monte Carlo (MCMC) methods are used to draw samples from probability distributions in a non-sequential setting. The advantages of MCMC over Importance Sampling (IS), which is the main principle used in particle filters, are that it is generally more effective in high-dimensional systems, and also easier to design for complex distributions. Recently, sequential MCMC schemes were proposed in the literature - see ([13], [14]) for a review. Although there are

no theoretical proofs of this yet, SMCMC has experimentally proven to be much more efficient than particle filtering (including particle filtering augmented with MCMC resample-moves [22]) at handling high-dimensional settings, because of the sequential nature of the algorithm allowing local exploration of the state-space with a single Markov chain at a given time step, thus reaching more relevant regions of the state-space in terms of posterior. On the contrary, a particle filter augmented with MCMC resample-moves will still suffer from the limitations of the importance sampling and resampling steps (which SMCMC omits entirely), and attempt to remedy them by constructing several independent Markov chains which is much less efficient than the SMCMC approach.

More specifically, the sequential MCMC (SMCMC) is a powerful sequential methodology for filtering that targets the joint posterior distribution defined in our case by (8). At a given time step, we use a MCMC procedure to make inference from this complex distribution (which is fixed for this time step). However, since we do not have a closed form representation of the posterior distribution $p(\mathbf{x}_{1:t-1,1:N}|\mathbf{y}^{1:M}_{1:t-1,1:N})$ at time $t-1$, it will be approximated by an empirical distribution based on the current particle set:

$$p(\mathbf{x}_{1:t-1,1:N}|\mathbf{y}^{1:M}_{1:t-1,1:N}) \approx \frac{1}{N_p}\sum_{j=1}^{N_p}\delta_{\mathbf{x}^{(j)}_{1:t-1,1:N}}(\mathbf{x}_{1:t-1,1:N}) \quad (12)$$

where N_p is the number of particles and (j) the particle index. Then, by plugging this particle approximation into (8), we obtain

$$\pi(\mathbf{x}_{1:t,1:N}) \propto \frac{1}{N_p}\sum_{j=1}^{N_p}\left(\prod_{i=1}^{M} p(\mathbf{y}^i_{t,1:N}|\mathbf{y}^i_{1:t-1,1:N}, \mathbf{x}^{(j)}_{1:t-1,1:N}, \mathbf{x}_{t,1:N})\right) \times p(\mathbf{x}_{t,1:N}|\mathbf{x}^{(j)}_{t-1,1:N})\delta_{\mathbf{x}^{(j)}_{1:t-1,1:N}}(\mathbf{x}_{1:t-1,1:N}) \quad (13)$$

where $\pi(\mathbf{x}_{1:t,1:N})$, an empirical approximation of the true posterior $p(\mathbf{x}_{1:t,1:N}|\mathbf{y}^{1:M}_{1:t,1:N})$ based on the particle set $\mathbf{x}^{(1:N_p)}_{1:t-1,1:N}$, is the target distribution of the Markov chain at time step t. At a given iteration n of the Markov chain, the variables $\mathbf{x}_{1:t-1,1:N}$ are to be drawn according to a uniform discrete distribution (selected uniformly from the set $\mathbf{x}^{(1:N_p)}_{1:t-1,1:N}$) whereas $\mathbf{x}_{t,1:N}$ is then drawn from a continuous distribution conditional to this previous sample, hence the designation "Joint Draw" for this procedure.

Then, having made many joint draws from (13) using an appropriate MCMC scheme, the converged MCMC output for variable $\mathbf{x}_{1:t,1:N}$ can be extracted to give an updated particle approximation of $p(\mathbf{x}_{1:t,1:N}|\mathbf{y}^{1:M}_{1:t,1:N})$ to be used at the next time iteration. More specifically, after a burn-in period of N_{burn}, keep every MCMC output $\mathbf{x}^{(j)}_{1:N} = \mathbf{x}^{n}_{1:N}$ as the new particle set for the posterior distribution (the notation (j) is meant to include only the N_p particles that are considered to be after the burn-in period, while n may refer to any particle of the chain). In this way, sequential inference can be achieved.

In addition to this procedure, we choose to perform an additional refinement step in order to improve the quality of the samples corresponding to time t. Several block sampling structures could be considered [23], but in this paper, we opt to sample successively each of the individual targets using a series of Metropolis-within Gibbs steps, which consists in drawing new samples component-wise, that is in our application, target-wise, conditionally to all other targets, and choosing whether to accept them. This allows to carefully move each component of our particles towards more interesting regions of the state-space, using densities that are focused on each component as opposed to the joint density used in the previous step. It should be emphasized that our block sampling Gibbs step is in fact target-wise and thus multivariate, rather than univariate coordinate-wise. This is much more efficient since in our setting there is a strong correlation between coordinates of a single target, which means sampling a single coordinate conditionally to other coordinates of the same target would be degenerated (close to deterministic).

To further take advantage of this approach, we also use a Langevin-type gradient proposal density for sampling in the refinement (this aspect will be detailed in Section IV). It is interesting to note that performing both a MH Joint Draw and next a component-wise Gibbs refinement is complementary. Indeed, the Gibbs step improves upon the previous joint sampling. However, if we were to omit the initial Joint Draw and only perform this refinement step, the sampling might become degenerated if there is high correlation between targets' measurements since we use a density conditional on all targets other than the current component [12]. Additionally, while in our chosen algorithm we only perform a single MH Joint Draw step, several iterations could potentially help improve the mixing for the Markov Chain [24] (once again especially when there is strong correlation between blocks, which in our case would correspond to targets in close proximity).

In short, at time t and at the n-th MCMC iteration, the following procedure is thus performed to obtain samples from $p(\mathbf{x}_{1:t,1:N}|\mathbf{y}^{1:M}_{1:t,1:N})$:

- Make a joint draw for $\mathbf{x}_{1:t,1:N}$ using a Metropolis-Hastings step,
- Refine the hidden state at current time t, $\mathbf{x}_{t,1:N}$, using a series of Metropolis-Hastings-within-Gibbs steps.

The complete proposed algorithm is summarized in Algorithm 1 (which also includes the Langevin-type gradient proposal explained in Section IV).

Following the acquisition of this set of particles (selected after a burn-in period) asymptotically drawn according to the density $p(\mathbf{x}_{1:t,1:N}|\mathbf{y}^{1:M}_{1:t,1:N})$, the target state estimation at time t can be performed using the minimum mean square error criterion as the mean of the particles, which corresponds to the empirical approximation of the expectation of the marginalized posterior density $p(\mathbf{x}_{t,1:N}|\mathbf{y}^{1:M}_{1:t,1:N})$:

$$\hat{\mathbf{x}}_{t,1:N} = \int \mathbf{x}_{t,1:N} p(\mathbf{x}_{t,1:N}|\mathbf{y}^{1:M}_{1:t,1:N}) d\mathbf{x}_{t,1:N} \approx \frac{1}{N_p}\sum_{j=1}^{N_p}\mathbf{x}^{(j)}_{t,1:N}. \quad (14)$$

Algorithm 1: Proposed SMCMC for Multi-Target Tracking.

At time t, to compute the n-th SMCMC particle trajectory $\mathbf{x}^n_{1:t,1:N}$:

Data: $\mathbf{y}^{1:M}_{1:t,1:N}$ (all of the measurements available at time t), $\mathbf{x}^{(1:N_p)}_{1:t-1,1:N}$ (the particle set constituting the empirical approximation of the posterior density from time $t-1$), $\mathbf{x}^{n-1}_{1:t,1:N}$ (the result of the previous step $n-1$ of the algorithm)

Joint Draw using Metropolis-Hastings

– Randomly select a joint particle trajectory $\tilde{\mathbf{x}}_{1:t-1,1:N}$ by sampling it from the empirical measure of $p(\mathbf{x}_{1:t-1,1:N}|\mathbf{y}^{1:M}_{1:t-1,1:N})$ obtained at the previous time iteration:

$$\tilde{\mathbf{x}}_{1:t-1,1:N} \sim \frac{1}{N_p}\sum_{j=1}^{N_p}\delta_{\mathbf{x}^{(j)}_{1:t-1,1:N}}(\mathbf{x}_{1:t-1,1:N}) \tag{15}$$

– Draw a random sample for the current t-th time step:

$$\tilde{\mathbf{x}}_{t,1:N} \sim p(\cdot|\tilde{\mathbf{x}}_{t-1,1:N}) \tag{16}$$

– Calculate the acceptance ratio which compares the likelihood given $\tilde{\mathbf{x}}_{1:t,1:N}$ with the likelihood given $\mathbf{x}^{n-1}_{1:t,1:N}$ (which is the one from the previous iteration $n-1$):

$$\alpha = \min\left(1, \frac{\prod_{i=1}^{M} p(\mathbf{y}^i_{t,1:N}|\mathbf{y}^i_{1:t-1,1:N}, \tilde{\mathbf{x}}_{1:t,1:N})}{\prod_{i=1}^{M} p(\mathbf{y}^i_{t,1:N}|\mathbf{y}^i_{1:t-1,1:N}, \mathbf{x}^{n-1}_{1:t,1:N})}\right) \tag{17}$$

– Accept this proposed particle or reject it:
draw $a \sim \mathcal{U}[0,1]$
if $(a < \alpha)$ **then**
  accept the particle, thus $\mathbf{x}^n_{1:t,1:N} := \tilde{\mathbf{x}}_{1:t,1:N}$
else
  reject the particle, thus $\mathbf{x}^n_{1:t,1:N} := \mathbf{x}^{n-1}_{1:t,1:N}$
end

Refinement using Metropolis-within-Gibbs

– Successively sample each target:
for $b = 1$ **to** N **do**
  – Define $\tilde{\mathbf{x}}_{1:t,1:N} := \mathbf{x}^n_{1:t,1:N}$
  – Draw a new sample from the gradient-based proposal density q in (19), for the b-th target at current time t:

$$\tilde{\mathbf{x}}_{t,b} \sim q(\cdot|\mathbf{x}^n_{t,b}) \tag{18}$$

  – Calculate the acceptance ratio as $\alpha = \min(1, \beta)$ where β is from (28), with the modified particle $\tilde{\mathbf{x}}_{1:t,1:N}$.
  – Accept this proposal particle or reject it:
  draw $a \sim \mathcal{U}[0,1]$
  if $(a < \alpha)$ **then**
    accept the particle, $\mathbf{x}^n_{t,b} = \tilde{\mathbf{x}}_{t,b}$
  else
    reject the particle, do not update the b-th block in $\mathbf{x}^n_{t,1:N}$
  end
end
Output: Sample $\mathbf{x}^n_{1:t,1:N}$

IV. Gradient-Based Proposal Density

The choice of a relevant proposal density to propagate the kinematic states in the Metropolis-within-Gibbs refinement steps is crucial for the algorithm to be able to "lock-on" to the targets. In our case, using the prior probability density may be prone to failure especially in scenarios where this density has a large covariance matrix. Therefore, we aim to overcome this problem using a proposal density that is dependent on the observations, so as to guide the particles towards regions of the state-space which harbor high likelihood.

We choose a Langevin-type ([25], [26]) proposal density $q(\cdot)$ which is based on the gradient of the target density (which includes the likelihood). For a target k, at the n-th step of the Metropolis-Hastings algorithm, the Gibbs refinement sample will be drawn as follows:

$$\tilde{\mathbf{x}}_{t,k} \sim q(\cdot|\mathbf{x}^n_{t,k}) = \mathcal{N}\left(\mathbf{x}^n_{t,k} + \mathbf{m}, \boldsymbol{\Sigma}\right) \tag{19}$$

where $\mathbf{x}^n_{t,k}$ results from the Metropolis-Hastings Joint Draw, and

$$\mathbf{m} = \frac{h}{2}\nabla\left(\log\Pi(\mathbf{x}_{t,k})\right)\Big|_{\mathbf{x}_{t,k}=\mathbf{x}^n_{t,k}}$$
$$\boldsymbol{\Sigma} = h\mathbf{I}_{\mathbf{4}\times\mathbf{4}}, \tag{20}$$

h being a step which needs to be chosen empirically so that the performance of the algorithm is optimal, and $\Pi(\mathbf{x}_{t,k})$, proportional to the conditional posterior density $p(\mathbf{x}_{t,k}|\mathbf{y}^{1:M}_{1:t,1:N}, \mathbf{x}^n_{1:t-1,1:N}, \mathbf{x}^n_{t,1:N\setminus k})$ for the current target of interest, being the product of the corresponding likelihood and prior terms, derived from (8); thus

$$\Pi(\mathbf{x}_{t,k}) = \prod_{i=1}^{M} p(\mathbf{y}^i_{t,1:N}|\mathbf{y}^i_{1:t-1,1:N}, \mathbf{x}^n_{1:t-1,1:N}, \mathbf{x}^n_{t,1:N\setminus k}, \mathbf{x}_{t,k}) \times p(\mathbf{x}_{t,k}|\mathbf{x}^n_{t-1,1:N}, \mathbf{x}^n_{t,1:N\setminus k}). \tag{21}$$

Using (9) and (10),

$$\log\Pi(\mathbf{x}_{t,k}) = \sum_{i=1}^{M}\log\mathcal{N}\left(\mathbf{y}^i_{t,1:N}; \boldsymbol{\mu}^i_t, \boldsymbol{\Sigma}^i_t\right) \tag{22}$$
$$+ \log p(\mathbf{x}_{t,k}|\mathbf{x}^n_{t-1,1:N}, \mathbf{x}^n_{t,1:N\setminus k}). \tag{23}$$

We need to calculate the gradient of

$$\log\mathcal{N}\left(\mathbf{y}^i_{t,1:N}; \boldsymbol{\mu}^i_t, \boldsymbol{\Sigma}^i_t\right) = -\frac{1}{2}\log 2\pi - \log|\boldsymbol{\Sigma}^i_t| - \frac{1}{2}\left(\mathbf{y}^i_{t,1:N} - \boldsymbol{\mu}^i_t\right)^T \times \boldsymbol{\Sigma}^i_t\left(\mathbf{y}^i_{t,1:N} - \boldsymbol{\mu}^i_t\right) \tag{24}$$

with respect to $\mathbf{x}_{t,k}$ and evaluate it at $\mathbf{x}^n_{t,k}$. In this expression, both $\boldsymbol{\mu}^i_t$ and $\boldsymbol{\Sigma}^i_t$ are dependent on $\mathbf{x}_{t,k}$ (see (10) and (11)). In order to simplify this problem, we assume all terms related to covariances (thus $\boldsymbol{\Sigma}^i_t$ as well as the covariance terms in $\boldsymbol{\mu}^i_t$) to be constant for the derivative. Under this assumption, denoting $A = \left(y^i_{t,1:N} - \mu^i_t\right)$ and $S = \Sigma^i_t$, we calculate for each component c

of $\mathbf{x}_{t,k} = [x_{t,k,x}, x_{t,k,y}, x_{t,k,\dot{x}}, x_{t,k,\dot{y}}]^T$ (thus $c \in \{x, y, \dot{x}, \dot{y}\}$):

$$\frac{\partial \mathbf{A}^{\mathbf{T}}\mathbf{S}\mathbf{A}}{\partial x_{t,k,c}} = \left(\frac{\partial \mathbf{A}^{\mathbf{T}}\mathbf{S}\mathbf{A}}{\partial \boldsymbol{\mu}_t^i}\right)^T \frac{\partial \boldsymbol{\mu}_t^i}{\partial x_{t,k,c}} \tag{25}$$

with

$$\frac{\partial \mathbf{A}^{\mathbf{T}}\mathbf{S}\mathbf{A}}{\partial \boldsymbol{\mu}_t^i} = -2\mathbf{S}\mathbf{A}$$

$$\frac{\partial \boldsymbol{\mu}_t^i}{\partial x_{t,k,c}} = \left[0, \cdots, 0, \frac{\partial f^i(\mathbf{x}_{t,k})}{\partial x_{t,k,c}}, 0, \cdots, 0,\right]^T (k\text{-th component}) \tag{26}$$

because all terms dependent on targets other than the k-th target have derivatives equal to 0. Moreover, the only term derived in $\boldsymbol{\mu}_t^i$ is $\boldsymbol{\mu}_2$ (from (11)), according to our assumption, since the only other term in $\boldsymbol{\mu}_t^i$ that depends on $\mathbf{x}_{t,k}$ is a covariance (namely $\boldsymbol{\Sigma}_{2,1}$). On the other hand,

$$\frac{\partial f^i(\mathbf{x}_{t,k})}{\partial \mathbf{x}_{t,k}} = \begin{bmatrix} \frac{\partial f^i(\mathbf{x}_{t,k})}{\partial x_{t,k,x}} \\ \frac{\partial f^i(\mathbf{x}_{t,k})}{\partial x_{t,k,y}} \\ \frac{\partial f^i(\mathbf{x}_{t,k})}{\partial x_{t,k,\dot{x}}} \\ \frac{\partial f^i(\mathbf{x}_{t,k})}{\partial x_{t,k,\dot{y}}} \end{bmatrix} = \begin{bmatrix} 10\alpha \frac{\left(x_{t,k,x} - s_x^i\right)}{\left(x_{t,k,x} - s_x^i\right)^2 + \left(x_{t,k,y} - s_y^i\right)^2} \\ 10\alpha \frac{\left(x_{t,k,y} - s_y^i\right)}{\left(x_{t,k,x} - s_x^i\right)^2 + \left(x_{t,k,y} - s_y^i\right)^2} \\ 0 \\ 0 \end{bmatrix} \tag{27}$$

the derivatives with respect to velocities being zero since the observations are only dependent on the distances between targets, thus only on target positions. Thus the propagation of velocity values is handled by the prior component alone. The derivative of this prior component is calculated in a similar way, except no assumptions are necessary.

Lastly, the expression of the acceptance ratio for the refinement step needs to be updated as it is dependent on the proposal density q (with the same notations as Algorithm 1):

$$\beta = \frac{\prod_{i=1}^M p(\mathbf{y}_{t,1:N}^i | \mathbf{y}_{1:t-1,1:N}^i, \tilde{\mathbf{x}}_{1:t,1:N})}{\prod_{i=1}^M p(\mathbf{y}_{t,1:N}^i | \mathbf{y}_{1:t-1,1:N}^i, \mathbf{x}_{1:t,1:N}^n)} \times \frac{p(\tilde{\mathbf{x}}_{t,k} | \mathbf{x}_{t-1,1:N}^n, \mathbf{x}_{t,1:N\setminus k}^n)}{p(\mathbf{x}_{t,k}^n | \mathbf{x}_{t-1,1:N}^n, \mathbf{x}_{t,1:N\setminus k}^n)} \frac{q(\mathbf{x}_{t,k}^n | \tilde{\mathbf{x}}_{t,k})}{q(\tilde{\mathbf{x}}_{t,k} | \mathbf{x}_{t,k}^n)}. \tag{28}$$

V. Simulation Results

In order to illustrate the performance improvements induced by

- using a SMCMC approach compared to a classical particle filtering approach (Section V-A with a figure showing the superiority of SMCMC the higher the dimension of the state-space is),
- replacing the prior proposal density with the gradient proposal density (Sections V-B and V-C with figures showing the varying amounts of performance gains depending on shadowing noise variance and number of particles),

we assume that each target evolves independently from the others in a field of 16 sensors as illustrated in Fig. 1, according to a nearly constant velocity model [27], [28] which is defined as follows for the j-th target:

$$\mathbf{x}_{t,j} = \mathbf{F}_t \mathbf{x}_{t-1,j} + \mathbf{u}_{t,j} \tag{29}$$

where $\mathbf{F}_t$ would be a 4×4 transition matrix and $\mathbf{u}_{t,j}$ a vector of independent realizations of $\mathcal{N}(\mathbf{0}_4, \mathbf{Q}_t)$ with $\mathbf{Q}_t$ a 4×4 state noise covariance matrix, both $\mathbf{F}_t$ and $\mathbf{Q}_t$ depending only on the time interval between t and $t-1$. Here $\mathbf{F}_t$ and $\mathbf{Q}_t$ are defined as:

$$\mathbf{F}_t = \begin{bmatrix} \mathbf{I}_2 & \tau_t \mathbf{I}_2 \\ \mathbf{0}_2 & \mathbf{I}_2 \end{bmatrix}, \mathbf{Q}_t = \sigma_{target} \begin{bmatrix} (\tau_t^3/3)\mathbf{I}_2 & (\tau_t^2/2)\mathbf{I}_2 \\ (\tau_t^2/2)\mathbf{I}_2 & \tau_t \mathbf{I}_2 \end{bmatrix} \tag{30}$$

with τ_t the time interval between two time steps, which is chosen constant and equal to 1 second, and $\sigma_{target}^2 = 10\ \mathrm{m}^2$.

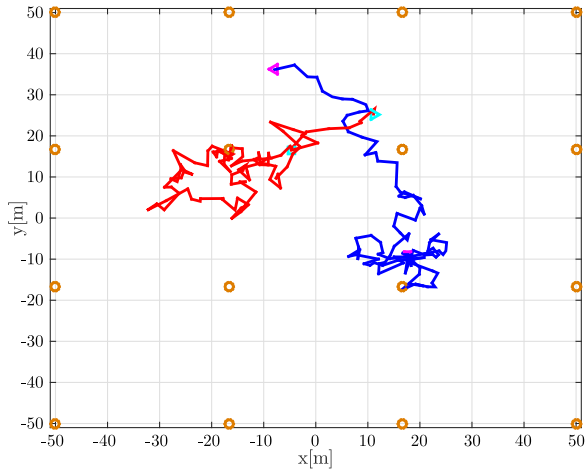

Fig. 1. Example of two chaotic trajectories with $\sigma_{target}^2 = 10\ \mathrm{m}^2$. The orange circles represent the sensors, the lines represent the trajectories and the □/△ symbols represent their starting/ending points, respectively.

Fig. 1 shows an example of two trajectories created with these parameters and chosen to be confined within a grid of sensors. Due to σ_{target}^2 having a relatively large value, the trajectories are chaotic, representing a difficult tracking scenario.

In order to assess the accuracy of the different algorithms when the measurements are randomly generated with standard deviation σ (for the shadowing noise) equal for all target-sensor links, we compute the root mean square error (RMSE) between the estimations and the real positions of the target (the estimations of other variables such as velocities or accelerations are not taken into account), in time, averaged on a number of Monte Carlo (MC) runs:

$$\mathrm{RMSE}_t = \sqrt{\frac{1}{N_{MC} N} \sum_{j=1}^{N} \sum_{l=1}^{N_{MC}} \|\hat{\mathbf{x}}_{t,j}^l - \mathbf{x}_{t,j}\|^2} \tag{31}$$

where $\hat{\mathbf{x}}_{t,j}^l$ is the estimated state of the j-th target from the l-th MC run. Throughout this section, we choose $N_{MC} = 10$, $N_{burn} = \frac{1}{10}$ and unless specified otherwise we keep a number

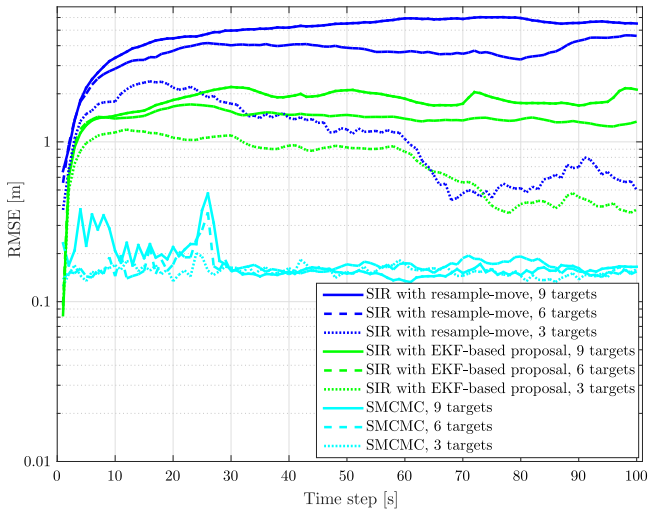

Fig. 2. Log-scale performance of our SMCMC algorithm versus a SIR algorithm with the same Gibbs refinement step as resample-move. Low measurement noise ($\sigma^2 = (0.1)^2$ dB) and process noise ($\sigma^2_{target} = 0.01\,\mathrm{m}^2$).

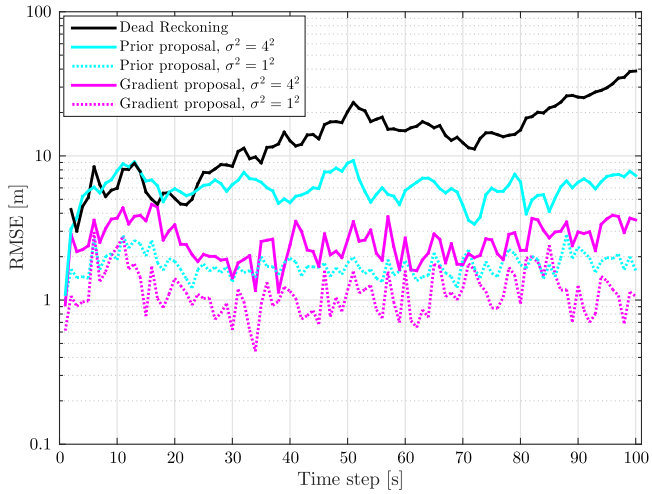

Fig. 3. Log-scale performance of the SMCMC algorithm using the gradient-based proposal density versus the prior density, for high measurement noise values on the chaotic trajectory set from Fig. 1 (difficult scenario).

of sensors $M = 16$, a number of targets $N = 2$ and a number of time steps $T = 100$. For reference, the experiments used Matlab software and a laptop featuring a 2.80 GHz Intel(R) Core(TM) i7-4810MQ CPU.

A. Performance Compared to Particle Filtering

First, we compare the proposed SMCMC algorithm with the particle filtering approach which was proposed in [10] in a similar context for single target tracking. More specifically, the particle filter used in this section is the Sequential Importance Resampling (SIR) [29] in which a resample-move strategy is employed after the resampling stage in order to diversify the set of particles [22]. This strategy uses exactly the same step described as the refinement step in our proposed SMCMC, including the gradient-based proposal, thus allowing for a fair comparison between the two algorithms. For further comparison we also implement a SIR without resample-move but instead using a custom EKF-based proposal [30]. Fig. 2 shows the RMSE obtained with all three algorithms in which $N_p = 200$ particles are used to do the inference, and the actual target trajectories are generated with $\sigma^2_{target} = 0.01$ m^2 thus much smoother than those from Fig. 1 (Section V-B below studies this more challenging case). In this simulation, the shadowing variance is $\sigma^2 = (0.1)^2$ dB which is a low noise in the context of our experiment, and different numbers of targets are used ($N = 3, 6, 9$). Indeed, the SIR algorithm's main weakness comes from the degeneration of the importance weights in situations where either the likelihood becomes too informative (with a too small variance) and no longer covers regions where the proposal distribution is high, or more interestingly in difficult situations where the state-space is high-dimensional. In such a multi-dimensional scenario, the results show the significant superiority of the proposed SMCMC against the SIR, with computational times of the same order; additionally, the average RMSE per target remains about the same for SMCMC as the total number of targets increases, while it deteriorates in the case of SIR. For reference, the computational time of this experiment with 3 targets, averaged over the MC runs and the time steps, is approximately 3.4144 seconds for SIR with resample-move, 1.6141 seconds for SIR with EKF-based proposal and 3.8601 seconds for SMCMC. The difference between SIR with resample-move and SMCMC corresponds almost exactly to an increase of 10% in the computational time, while the SMCMC method uses an additional burn-in period of precisely 10% of the total number of particles (in this case, 222 particles including the burn-in, compared to 200 for SIR with resample-move and for SMCMC without burn-in). Thus, SIR with resample-move and SMCMC have a similar computational time for a single particle (and the same remarks still apply with higher numbers of targets).

B. Performance in Difficult, Noisy Scenarios

We now demonstrate the benefits of using the gradient proposal distribution presented in Section IV instead of the basic prior proposal in our Gibbs refinement moves, in difficult scenarios. Given the chaotic hidden state trajectories from Fig. 1 (thus $N = 2$), and either $\sigma^2 = 1^2$ dB (average-to-high measurement noise) or $\sigma^2 = 4^2$ dB (high measurement noise), we run our algorithm with either the prior proposal density or the gradient proposal density from Section IV. Fig. 3 shows the resulting RMSE performance with respect to the time step, for $N_p = 500$. As expected, the estimator using the gradient proposal performs better. For reference, the computational time of this experiment, averaged over the MC runs and the time steps, is approximately 1.5205 second with the prior proposal and 3.2878 seconds with the gradient proposal, when $\sigma^2 = 1^2$ dB. When $\sigma^2 = 4^2$ dB, the computational times are 1.8128 second and 3.8967 seconds, respectively.

Still using this scenario, monitoring the relevance of the proposed particles through values of the acceptance ratio from the Gibbs refinement step in Table I shows that the gradient proposal allows to significantly reduce the rejection of samples due to this step, which is proof that the set of particles

TABLE I
ACCEPTANCE RATIOS IN THE GIBBS REFINEMENT STEP WHEN USING EITHER THE PRIOR PROPOSAL DENSITY OR THE GRADIENT-BASED ONE, WITH VARYING MEASUREMENT NOISE

	Prior	Gradient
$\sigma^2 = (0.1)^2$	0.0066	0.0392
$\sigma^2 = (0.3)^2$	0.0075	0.2669
$\sigma^2 = (1)^2$	0.0377	0.8198
$\sigma^2 = (2)^2$	0.1940	0.9117
$\sigma^2 = (4)^2$	0.4860	0.9500

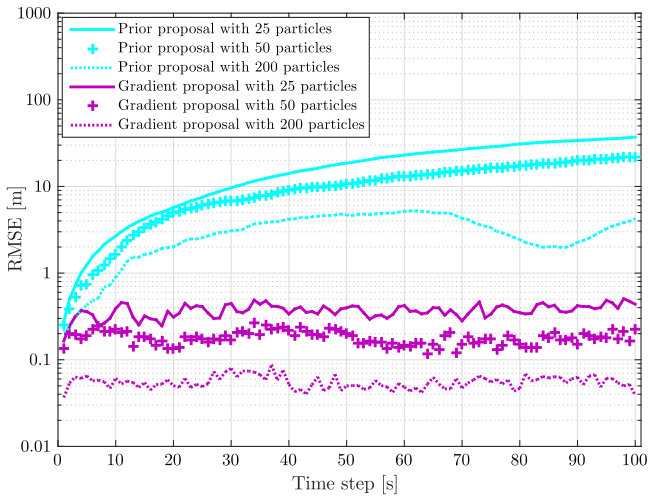

Fig. 4. Log-scale performance of the algorithm using the gradient-based proposal density versus the prior density, with low measurement noise ($\sigma^2 = (0.1)^2$dB) and average process noise ($\sigma^2_{target} = 1\text{m}^2$).

propagated is able to reach regions of the state-space featuring much higher likelihood than with the prior proposal. Moreover, from a theoretical point of view, the gain of performance due to using the gradient proposal should decrease when the measurement noise increases, since this density aims to guide the sampled particles towards these regions of high likelihood, because then such regions become very wide and inaccurate. Table I confirms that the gain in acceptance ratio indeed decreases when the measurement noise increases. Fig. 4 from Section V-C also confirms this by showing much larger performance gain with lower noise (and also less chaotic trajectories) than in Fig. 3's difficult scenario.

C. Performance in Easier Scenarios With Varying Number of Particles

Another benefit of using this gradient-based density can be demonstrated when reducing the number of particles used for the filter. Indeed, using the Gaussian prior density implies that in order to draw only a few particles which will be located in regions of interest where the likelihood function is high, it is required to draw a very large number of particles in total, whereas the gradient-based density has no such drawback (as the acceptance ratios from Table I also demonstrate). Fig. 4 shows RMSE values in time for different numbers of particles, displaying how the linear gap of performance between the two proposal densities increases when the number of particles used decreases. For reference, the computational time of this experiment, averaged over the MC runs and the time steps, is approximately 0.24 second when using 25 particles and 1.66 second when using 200 particles.

VI. CONCLUSIONS

This paper proposes a sequential MCMC solution to multitarget tracking with RSS measurements, taking into account spatio-temporal correlations between targets and using a gradient-based proposal density for drawing particles in the Gibbs refinement moves. The simulation results show a performance improvement (about 50% increase in accuracy) in any scenario compared to using the prior density as a proposal, and the gain is especially large (above 90%) when using low number of particles or when the model considered features informative measurements. The SMCMC approach is also shown to be superior to particle filtering in this setting when both use the same Gibbs refinement moves.

REFERENCES

[1] I. Guvenc and C.-C. Chong, "A survey on TOA based wireless localization and NLOS mitigation techniques," *IEEE Commun.. Surveys Tut.*, vol. 11, no. 3, pp. 107–124, Jul.–Sep. 2009.
[2] B. Van Veen and K. Buckley, "Beamforming: A versatile approach to spatial filtering," *IEEE Acoust., Speech, Signal Process. Mag.*, vol. 5, no. 2, pp. 4–24, Apr. 1988.
[3] N. Patwari, A. Hero, M. Perkins, N. Correal, and R. O'Dea, "Relative location estimation in wireless sensor networks," *IEEE Trans. Signal Process.*, vol. 51, no. 8, pp. 2137–2148, Aug. 2003.
[4] M. Gudmundson, "Correlation model for shadow fading in mobile radio systems," *Electron. Lett.*, vol. 27, no. 23, pp. 2145–2146, Nov. 1991.
[5] P. Agrawal and N. Patwari, "Correlated link shadow fading in multihop wireless networks," *IEEE Trans. Wireless Commun.*, vol. 8, no. 8, pp. 4024–4036, Aug. 2009.
[6] N. Salman, L. Mihaylova, and A. Kemp, "Localization of multiple nodes based on correlated measurements and shrinkage estimation," in *Proc. Sensor Data Fusion: Trends, Solutions, Appl.*, Oct. 2014, pp. 1–6.
[7] L. Mihaylova, D. Angelova, D. Bull, and N. Canagarajah, "Localization of mobile nodes in wireless networks with correlated in time measurement noise," *IEEE Trans. Mobile Comput.*, vol. 10, no. 1, pp. 44–53, Jan. 2011.
[8] L. Mihaylova, D. Angelova, S. Honary, D. Bull, C. Canagarajah, and B. Ristic, "Mobility tracking in cellular networks using particle filtering," *IEEE Trans. Wireless Commun.*, vol. 6, no. 10, pp. 3589–3599, Oct. 2007.
[9] B. Ferris, D. Hähnel, and D. Fox, "Gaussian processes for signal strength-based location estimation," in *Proc. Robot., Sci. Syst.*, 2006, pp. 1–8.
[10] H. Noureddine, N. Gresset, D. Castelain, and R. Pyndiah, "Auto-regressive modeling of the shadowing for RSS mobile tracking," in *Proc. IEEE Int. Conf. Commun.*, Jun. 2011, pp. 1–5.
[11] C. Snyder, T. Bengtsson, P. Bickel, and J. Anderson, "Obstacles to high-dimensional particle filtering," *Monthly Weather Rev., Special Collection, Math. Advances Data Assimilation*, vol. 136, no. 12, pp. 4629–4640, 2008.
[12] F. Septier, S. K. Pang, A. Carmi, and S. Godsill, "On MCMC-based particle methods for bayesian filtering: Application to multitarget tracking," in *Proc. 3rd IEEE Int. Workshop Comput. Advances Multi-Sensor Adaptive Process*, Dec. 2009, pp. 360–363.
[13] A. Brockwell, P. Del Moral, and A. Doucet, "Sequentially interacting Markov chain Monte Carlo methods," *Ann. Statist.*, vol. 38, no. 6, pp. 3387–3411, Dec. 2010. [Online]. Available: http://dx.doi.org/10.1214/09-AOS747
[14] F. Septier and G. W. Peters, "An overview of recent advances in Monte-Carlo methods for Bayesian filtering in high-dimensional spaces," in *Theoretical Aspects Spatial-Temporal Modeling* (SpringerBriefs—JSS Research Series in Statistics), G. W. Peters and T. Matsui, Eds. Berlin, Germnay: Springer, Nov. 2015. [Online]. Available: https://hal-imt.archives-ouvertes.fr/hal-01198429

[15] R. Lamberti, F. Septier, N. Salman, and L. Mihaylova, "Sequential Markov Chain Monte Carlo for multi-target tracking with correlated RSS measurements," in *Proc. IEEE 10th Int. Conf, Intell. Sensors, Sensor Netw Inf. Process.*, Apr. 2015, pp. 1–6.
[16] K. Pahlavan and A. H. Levesque, *Wireless Information Networks*. New York, NY, USA: Wiley, 1995, vol. 95.
[17] T. Rappaport, *Wireless Communications: Principles and Practice (Electrical Engineering)*. Englewood Cliffs, NJ, USA: Prentice-Hall, 1996. [Online]. Available: https://books.google.fr/books?id=C_pSAAAAMAAJ
[18] I. Nevat, G. W. Peters, K. Avnit, F. Septier, and L. Clavier, "Location of things: Geospatial tagging for IoT using time-of-arrival," *IEEE Trans. Signal Inf. Process. over Netw.*, vol. 2, no. 2, pp. 174–185, Jun. 2016.
[19] N. Patwari, J. N. Ash, S. Kyperountas, A. O. Hero, R. L. Moses, and N. S. Correal, "Locating the nodes: Cooperative localization in wireless sensor networks," *IEEE Signal Process. Mag.*, vol. 22, no. 4, pp. 54–69, Jul. 2005.
[20] D. S. Baum, J. Hansen, and J. Salo, "An interim channel model for beyond-3G systems: Extending the 3GPP spatial channel model (SCM)," in *Proc. 61st IEEE Veh. Technol. Conf.*, vol. 5, May 2005, vol. 5, pp. 3132–3136.
[21] C. Snyder, "Particle filters, the optimal proposal and high-dimensional systems," in *Proc. Seminar Data Assimilation Atmosphere Ocean*. Shinfield Park, Reading, MA, USA: ECMWF, 2012, pp. 161–170.
[22] W. R. Gilks and C. Berzuini, "Following a moving target-Monte Carlo inference for dynamic Bayesian models," *J. Roy.l Statist. Soc. B (Statist. Methodology)*, vol. 63, pp. 127–146, 2001.
[23] G. O. Roberts and S. K. Sahu, "Updating schemes, correlation structure, blocking and parameterization for the Gibbs sampler," *J. Roy. Statist. Soc. B (Statist. Methodology)*, vol. 59, no. 2, pp. 291–317, 1997. [Online]. Available: http://dx.doi.org/10.1111/1467–9868.00070
[24] L. Martino, V. Elvira, and G. Camps-Valls, "The recycling gibbs sampler for efficient learning," arXiv:1611.07056, 2016.
[25] F. Septier and G. W. Peters, "Langevin and Hamiltonian based sequential MCMC for efficient Bayesian filtering in high-dimensional spaces," *IEEE J. Sel. Topics Signal Process.*, vol. 10, no. 2, pp. 312–327, Mar. 2016.
[26] M. Girolami and B. Calderhead, "Riemann manifold Langevin and Hamiltonian Monte Carlo methods," *J. Roy. Statist. Soc. B (Statist. Methodology)*, vol. 73, no. 2, pp. 123–214, 2011. [Online]. Available: http://dx.doi.org/10.1111/j.1467–9868.2010.00765.x
[27] X. Li and V. Jilkov, "Survey of maneuvering target tracking. Part I. Dynamic models," *IEEE Trans. Aerosp. Electron. Syst.*, vol. 39, no. 4, pp. 1333–1364, Oct. 2003.
[28] W. Blair, "Design of nearly constant velocity track filters for tracking maneuvering targets," in *Proc. 11th Int. Conf. Inf. Fusion*, Jun. 2008, pp. 1–7.
[29] A. Doucet, N. De Freitas, and N. Gordon, Eds., *Sequential Monte Carlo Methods in Practice*. Berlin, Germany: Springer-Verlag, 2001.
[30] A. Doucet, S. Godsill, and C. Andrieu, "On sequential Monte Carlo sampling methods for Bayesian filtering," *Statist. Comput.*, vol. 10, no. 3, pp. 197–208, Jul. 2000. [Online]. Available: http://dx.doi.org/10.1023/A:1008935410038

Roland Lamberti received the M.Sc. degree in telecom engineering from Telecom SudParis, Evry, France, in 2015. He is currently working toward the Ph.D. degree in the Department of Communications, Images and Information Processing, Telecom SudParis, on the subject of high-dimensional Bayesian inference.

François Septier received the Engineer degree in electrical engineering and signal processing from Télécom Lille, France, in 2004 and the Ph.D. degree in electrical engineering from the University of Valenciennes, Valenciennes, France, in 2008. From March 2008 to August 2009, he was a Research Associate in the Signal Processing and Communications Laboratory, Engineering Department, Cambridge University, Cambridge, U.K. Since August 2009, he is an Associate Professor with the IMT Lille Douai/CRIStAL UMR CNRS 9189, France. His research focuses on Bayesian computational methodology with a particular emphasis on the development of Monte Carlo based approaches for complex and high-dimensional problems.

Naveed Salman received the Bachelor's degree with Honours in electrical and electronics engineering from NWFP University of Engineering and Technology, Peshawar, Pakistan, in 2007 and the Master's and PhD degrees from the University of Leeds, Leeds, U.K., in 2009 and 2014 respectively. From 2014 to 2016, he was a Research Associate in the Department of Automatic Control and Systems Engineering, University of Sheffield, Sheffield, U.K. He is currently working in collaboration with Nestle U.K. Ltd., Gatwick, U.K., on the Innovate UK project "Effective milk processing with variable composition" at the National Centre of Excellence for Food Engineering, Sheffield Hallam University, Sheffield, U.K. He is the author of a number of journal and conference papers and is the recipient of the 2012 GW Carter best paper award from Leeds University. He also serves as a Reviewer for several international journals and conferences including the IEEE TRANSACTION ON WIRELESS COMMUNICATIONS, the IEEE TRANSACTION ON COMMUNICATIONS, the IEEE WIRELESS COMMUNICATIONS LETTERS, and IEEE COMMUNICATIONS LETTERS.

Lyudmila Mihaylova (SM'08) is a Professor of signal processing and control in the Department of Automatic Control and Systems Engineering, University of Sheffield, Sheffield, U.K. Her research interests include machine learning and autonomous systems with various applications such as intelligent transportation systems, navigation, surveillance, and sensor network systems. She has given a number of talks and tutorials, including the plenary talk for the IEEE Sensor Data Fusion 2015 (Germany), invited talks University of California, Los Angeles, IPAMI Traffic Workshop 2015 (USA), IET ICWMMN 2013 in Beijing, China. She is an Associate Editor of the IEEE TRANSACTIONS ON AEROSPACE AND ELECTRONIC SYSTEMS and of the *Elsevier Signal Processing Journal*. She was elected in March 2016 as the President of the International Society of Information Fusion (ISIF). She is on the board of Directors of ISIF. She was the General Co-Chair IET Data Fusion & Target Tracking 2014 and 2012 Conferences, Program Co-Chair for the 19th International Conference on Information Fusion, Heidelberg, Germany, 2016, and Academic Chair of Fusion 2010 conference.